On the Use of the Generalized Autocatalytic Models: The Thermal Decomposition of 3,5-dinitro-4-Methylbenzoic Acid

Roberto Sanchirico
Istituto di Ricerche sulla Combustione (IRC) – Consiglio Nazionale delle Ricerche (CNR), P.le V. Tecchio, 80 - 80125 Napoli, Italy

DOI 10.1002/aic.14729
Published online January 12, 2015 in Wiley Online Library (wileyonlinelibrary.com)

The thermal decomposition of 3,5-dinitro-4-methylbenzoic acid is studied by means of differential calorimetric techniques (DSC). Its autocatalytic behaviour has been highlighted and the decomposition process has been described considering the generalized expression of the Šesták–Berggren model. A new procedure for the optimization of the initiation parameter along with the other Arrhenius constants and kinetic exponents starting from the knowledge of the classic Šesták–Berggren model is illustrated. Encouraging results point out the validity of the approach which has been verified considering both a series of numerical and real experiments. © 2015 American Institute of Chemical Engineers *AIChE J*, 61: 1300–1308, 2015

Keywords: reaction kinetics, safety, generalized autocatalysis, 3, 5-dinitro-4-methylbenzoic acid, differential scanning calorimetry

Introduction

The assessment and the associated modelling of autocatalytic processes play a fundamental role in the context of a safety analysis.[1,2] Thermal unstable compounds or reacting mixtures capable to undergo exothermal decomposition phenomena with a huge heat release and gas evolution have been responsible for catastrophic events during the past[3–5] and this despite extensive work devoted to their study. A literature survey clearly indicates that one of the major causes of these incidents can be ascribed to the lack of knowledge of the phenomena involved. One of the most dangerous errors that can lead to unpredictable or uncontrollable situations is the wrong or partial characterization of the thermokinetic aspects involved during the thermal decomposition under study. The possibility of discriminating among autocatalytic and reaction order processes is fundamental and represent the first step that leads to a correct kinetic analysis which is fundamental for safety evaluations. It has been recently shown[6] that two dynamic differential scanning calorimetric (DSC) runs allow us to discriminate among the Šesták–Berggren[7,8] (Eq. 1) model (autocatalytic)

$$\mathrm{SB}(p,q) : f(\alpha)=\alpha^{p}(1-\alpha)^{q} \tag{1}$$

and reaction order model (Eq. 2)

$$\mathrm{RO}(v) : f(\alpha)=(1-\alpha)^{v} \tag{2}$$

while a set of three of these runs provide a complete kinetic analysis allowing the assessment of the whole kinetic triplet [A E f(α)]. This approach has been recently used for the prediction of the onset temperature and other important adiabatic parameters.[9] Of course, other methodologies can be considered for the characterization of the thermal decomposition under study. One of these approaches involves the analysis of the isothermal heat power profile.[10] A strictly decreasing shape of these curves indicates a *reaction order* behaviour while the presence of a maximum is characteristic of *autocatalytic* processes. However, sometimes it is very difficult to characterize the nature of the phenomenon under study by means of the isothermal techniques due to the confusing behaviour that is often registered especially during the initial tract of an isothermal curve. Another drawback can be found in the duration of the isothermal experiments that could require long experiments carried out over time scales varying from few hours to days or weeks, depending on the temperature. Although a precautionary approach should be in order especially during a safety analysis by pooling different information gathered using different experimental techniques, the resulting experimental plan could be very extensive thus preventing its practical implementation. This suggests maximizing the use of limited basic information available by means of reliable theoretical tools during the preliminary evaluation stage.

The practical use of the autocatalytic Šesták–Berggren's model (Eq. 1) can be difficult due to the fact that for the integration of the mass balance equation (Eq. 3), an initial value of the conversion different than zero is required:$\alpha(0)=\alpha_0 \neq 0$

$$\frac{d\alpha}{dt}=K(T)f(\alpha) \tag{3}$$

This means that the thermal history of the sample until the initial condition is reached has to be known and the corresponding initial conversion should be estimated.[11] This is a strong limitation that has been overcome considering an apparent slightly modified form of Eq. 1[12]

Correspondence concerning this article should be addressed to Roberto Sanchirico at r.sanchirico@irc.cnr.it

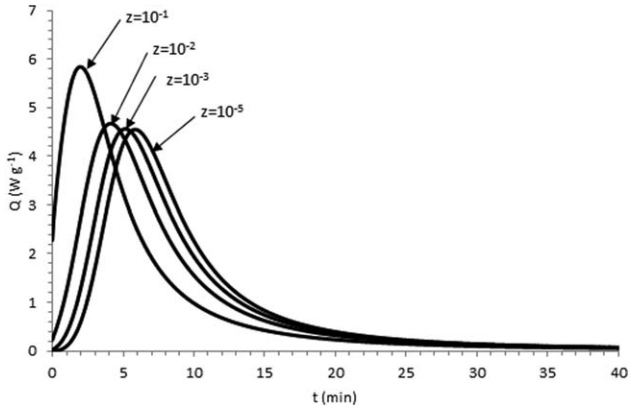

Figure 1. Simulated heat power curves gathered integrating the Eq. 5 under isothermal conditions ($T = 473.16$ K) with the GSB(z, m, n) model (Eq. 4) using different values (reported near the respective curve) of the initiation parameter z.

$$\mathrm{GSB}(z,m,n): f(\alpha)=(z+\alpha^m)(1-\alpha)^n \tag{4}$$

Equation 4 is generally referred to as generalized autocatalytic (GSB) model[12,13,15] and, provided that $z > 0$, lead to the integration of the mass balance equation (Eq. 3) assuming an initial conversion equal to zero [$\alpha(0)=\alpha_0=0$].

The use of the GSB model could be beneficial when for physical reasons the initial condition for the conversion should be considered equal to zero. An example of this situation occurs in the modelling of a tank or silos containing an unstable compound exposed to an external growing fire: for $t = 0$ the temperature of the bulk is the storage temperature and the initial conversion of the reacting system should be considered equal to zero. In these conditions, the integration of the heat and mass balance equations is not possible considering the SB equation whereas the GSB model can be applied successfully for solving the problem.

The approach described above is based on the assumption represented by Eq. 3, the so-called single step hypothesis.[14] This assumption, that allow us to write the reaction progress $\frac{d\alpha}{dt}$ as the product of two independent terms, the first depending only on temperature (kinetic constant with an Arrhenius structure: $K(T)=A\exp\left(-\frac{E}{RT}\right)$) and the second depending exclusively on the conversion degree [kinetic model: f(α)] lumps in a single step process the complex nature of the phenomenon under study and should be carefully verified before considering the use of semiempirical models like that reported in Eqs. 1, 2, and 4.

Equation 3 with the kinetic model given by Eq. 4 is generally integrated assigning to the parameter z a small value[15] or evaluated by means of trial and error procedures.[12] Figure 1 reports the heat power curves calculated under isothermal conditions at $T = 473.16$ K considering the Eq. 5

$$Q(t)=\frac{d\alpha}{dt}(-\Delta H_R)=K(T)f(\alpha)(-\Delta H_R) \tag{5}$$

evaluated considering the Eq. 4 for the kinetic model, with a reaction heat of $-\Delta H_R = 2500$ J g^{-1} and with the following values of the Arrhenius parameters: $A = 10^{+9}$ s^{-1}, $E = 10^{+5}$ J mol^{-1} and $m=\frac{3}{4}$ and $n = 2$ for the kinetic exponents.

As it is clearly pointed out by the behaviour of the response variable (heat power) against the variation of z, a high sensitivity has to be taken into account with respect to this parameter. Considering these limitations optimizing the initial value of parameter z along with all the other unknown parameters is significant and will be the matter of the present work.

Theoretical Considerations

The value of the parameter z (intended as initiation value) is often fixed *a priori* to small values. As shown above the kinetic model is very sensitive to changes in values of z.

If we consider a model fitting approach[6,16] using a multivariate ordinary least square (OLS) procedure, the problem that has to be solved is the assessment of the vector of parameters $\hat{\underline{\vartheta}}$ that minimize the sum of the squared errors Ψ evaluated considering all the experimental data available over the parameter space: $\hat{\underline{\vartheta}}=\arg\min_{\underline{\vartheta}}\Psi(\underline{\vartheta})$.

Let us suppose that the thermal decomposition process under study is showing an autocatalytic behavior. In the case of the extended Šesták–Berggren model (Eq. 4), the vector of parameters that has to be identified is $\underline{\vartheta}=[zA_{\mathrm{GSB}}\,E_{\mathrm{GSB}}\,mn]$. The success of the *model fitting* approach, due to the very complex nature of the objective function (that can show different local minima in a multidimensional Euclidean space), is strongly affected by the choice of the initial values of the parameters.

The procedure that assigns to z a small but arbitrary value allows us to determine a kinetic triplet corresponding to the minimum of the objective function, but these estimates could be different depending on the value of z taken into account. This mean that the result of the identification procedure carried out considering this approach could lead to different solutions preventing the reliable estimate of the kinetic triplet.

A possible strategy for the assessment of an initial estimate of the vector of parameters when $f(\alpha)$ is given by the Eq. 4 and the kinetic constant has an Arrhenius structure, is based on the knowledge of the kinetic triplet describing the experimental data derived considering for $f(\alpha)$ the classic SB(p, q) model given in Eq. 1. With the aim of identifying the SB(p,q) model, the method described in the Ref. 6 can be adopted. In this way, the experimental data will be supposed to be constituted by a set of three DSC runs carried out under dynamic conditions using three different heating rates and staring from the same initial temperature.

Let us suppose that both the model, SB(p, q) and GSB(z, m, n) can describe under the same thermal history and with the same precision the system under study, that is, let us suppose that there is a solution $\alpha = \alpha(t)$ of the differential problem built considering the classic SB(p, q) model (Eq. 1)

$$\begin{cases} \dfrac{d\alpha}{dt}=K_{\mathrm{SB}}(T)\alpha^p(1-\alpha)^q \\ \alpha(t_O)=\alpha_O \end{cases} \tag{6}$$

and a solution $\gamma = \gamma(t)$ of the differential problem built considering for the kinetic model the extended GSB(z, m, n)model (Eq. 4)

$$\begin{cases} \dfrac{d\gamma}{dt}=K_{\mathrm{GSB}}(T)(z+\gamma^m)(1-\gamma)^n \\ \gamma(t_O)=\gamma_O \end{cases} \tag{7}$$

such that $\alpha(t) = \gamma(t)$ $\forall t \geq t_O > 0$ (this imply that $\frac{d\alpha}{dt}=\frac{d\gamma}{dt}$ $\forall t \geq t_O$). This means that the second members of the Eqs. 6 and 7 are equal and then the following expression (Eq. 8) holds

$$K_{SB}(T)\alpha^p(1-\alpha)^q = K_{GSB}(T)(z+\gamma^m)(1-\gamma)^n \quad (8)$$

Rearranging Eq. 8 written for $t=t_O$ the following expression of z can be derived

$$z = \frac{K_{SB}(T)}{K_{GSB}(T)}\alpha_O{}^p(1-\alpha_O)^{q-n} - \alpha_O{}^m \quad (9)$$

The application of the extended Kissinger's method[17,18] (Eq. 14) shows that the two values of the activation energies have to be the same both for the SB(p,q) and the GSB(z, m, n) model: $E_{SB}=E_{GSB}$. This mean that the ratio: $\frac{K_{SB}(T)}{K_{GSB}(T)}$ can be rewritten as follow:

$$\frac{K_{SB}(T)}{K_{GSB}(T)} = \frac{A_{SB}\exp\left(-\frac{E_{SB}}{RT}\right)}{A_{GSB}\exp\left(-\frac{E_{GSB}}{RT}\right)} = \frac{A_{SB}}{A_{GSB}}$$

.

Substituting this last expression in Eq. 9 we get

$$z = \frac{A_{SB}}{A_{GSB}}\alpha_O{}^p(1-\alpha_O)^{q-n} - \alpha_O{}^m \quad (10)$$

Taking into account the heat powers expressed as a function of the temperature: $q_i(T)=K(T)f(\alpha)(-\Delta H_R)$ written for two different values of the heating rates $i \neq j$, it can be easily concluded that the exponents q and n have to be the same. In fact, considering the logarithm of the ratio of these heat powers, written both in the case of SB(p, q) and GSB(z, m, n), we get

$$\ln\left(\frac{Q_i}{Q_j}\right) = \begin{cases} \ln\left(\frac{\alpha_i^p}{\alpha_j^p}\right) + q\ln\left(\frac{1-\alpha_i}{1-\alpha_j}\right) & \text{(for the SB}(p,q)\text{model)} \\ \ln\left(\frac{z+\alpha_i^m}{z+\alpha_j^m}\right) + n\ln\left(\frac{1-\alpha_i}{1-\alpha_j}\right) & \text{(for the GSB}(z,m,n)\text{model)} \end{cases}$$

If we consider the plot $\ln\left(\frac{Q_i}{Q_j}\right)$ vs. $\ln\left(\frac{1-\alpha_i}{1-\alpha_j}\right)$comparing the second members of the above equations it can be easily concluded that $q = n$ and thus the expression in Eq. 10 can be written as

$$z = \alpha_O{}^p(r - \alpha_O{}^{m-p}) \quad (11)$$

where r is defined as

$$r = \frac{A_{SB}}{A_{GSB}} \quad (12)$$

Equation 11 and the definition of the parameter r (Eq. 12) represent the new scaling rules that will be considered along with the classic scaling and centering of the kinetic constant (Eq. 15) during the OLS procedure for the assessment of the kinetic triplet in the case of GSB model.

It has been shown that, if the single step hypothesis is verified, a set of three Dynamic DSC runs carried out under different heating rates provides a complete description of the system under study. In particular, it has been demonstrated that if two DSC heat power curves $Q = Q(T)$ at two different heating rates intercept in a point different than the origin, the behaviour of the system can be described using the SB(p, q) model; this circumstance exclude the validity of the RO(v) model pointing out the autocatalytic nature of the process under study.[6]

The linear interpolation of the variable defined using the Eqs. 13a and 13b

$$x_{i,j} = \frac{\ln\left(\frac{1-\alpha_i}{1-\alpha_j}\right)}{\ln\left(\frac{\alpha_i}{\alpha_j}\right)} \quad (13a)$$

$$y_{i,j} = \frac{\ln\left(\frac{q_i}{q_j}\right)}{\ln\left(\frac{\alpha_i}{\alpha_j}\right)} \quad (13b)$$

evaluated for the different combination of indexes $(i,j) = (1,2)$, $(2,3)$, and $(1,3)$ over suitable temperature intervals provide a first estimate of the kinetic exponent p and q which are calculated as the mean values, respectively, of the intercepts and slopes of these lines

$$y_{i,j} = p + q x_{i,j} \quad (13c)$$

Once obtained, these estimates are used to evaluate the derivative $f'(\alpha)$ of $f(\alpha)$,and then, applying the extended Kissinger method, to gather a first estimate of the Arrhenius parameters: this require at least three experimental DSC dynamic runs gathered using different heating rate $\beta_1 < \beta_2 < \beta_3$

$$\ln\left(\frac{\beta_i}{T_{i,max}^2}\right) = -\frac{E}{RT_{i,max}} + \ln\left(\frac{AR}{E}\xi(\alpha_{i,max})\right)(i=1,2,3) \quad (14)$$

where $\xi(\alpha_{i,max}) = -\left[\frac{df(\alpha)}{dT}\right]_{\alpha_{i,max}}$. Using the Eq. 14, from the plot $\ln\left(\frac{\beta_i}{T_{i,max}^2}\right)$ vs. $\frac{1}{T_{i,max}}$ it is possible to determine a first estimate of the activation energy $E_{SB,O}$, from the slope and the pre-exponential factor $A_{SB,O}$ from intercept of this line.

In the successive steps, due to the extreme stiffness of the optimization of the Arrhenius parameters A and E, a reparametrized expression of the kinetic constant (Eq. 15) is considered[19]

$$K(T) = \exp\left[c - d\frac{E_0}{R}\left(\frac{1}{T} - \frac{1}{T_{Ref}}\right)\right] \quad (15)$$

where T_{Ref} is a reference temperature calculated as the mean value between the temperature at the first inflection point of the peak at lowest heating rate and the temperature at the second inflection point at the highest heat rate. With this assumption, the new parameters that have to be identified are $\underline{\vartheta'} = [c_{SB}, d_{SB}, p, q]$. The initial estimate $\underline{\vartheta'_0} = [c_{SB,O}, d_{SB,O}, p_O, q_O]$ is evaluated deriving $c_{SB,O}$ by means of the Eq. 16 setting $d = d_{SB,O} = 1$, $A_O = A_{SB,O}$ and $E_O = E_{SB,O}$

$$c = \ln(A_0) - \left(\frac{E_0 d}{RT_{Ref}}\right) \quad (16)$$

After the final estimate $\underline{\hat{\vartheta}}_{SB} = [\hat{c}_{SB}\hat{d}_{SB}\hat{p}\hat{q}]$ has been determined the corresponding Arrhenius parameters $\hat{E}_{SB}$ and $\hat{A}_{SB}$ are calculated by means of inverse transformations

$$E = dE_0 \quad (17)$$

$$A = \exp\left(c + \frac{E_0 d}{RT_{Ref}}\right) \quad (18)$$

setting $d = \hat{d}_{SB}$ and $c = \hat{c}_{SB}$.

In the hypothesis that the structure of generalized GSB is near that of the SB model the mass balance (Eq. 19) written

considering Eq. 11 with the reparametrized expression of the kinetic constant (Eq. 15)

$$\frac{d\gamma}{dt}=\exp\left[c-d\frac{E_0}{R}\left(\frac{1}{T}-\frac{1}{T_{\mathrm{Ref}}}\right)\right][\alpha_O\hat{p}(r-{\alpha_O}^{m-\hat{p}})+\gamma^m](1-\gamma)^n \tag{19}$$

is optimized considering the following initial values of the model parameters: $c_O=\hat{c}_{\mathrm{SB}}$, $d_O=\hat{d}_{\mathrm{SB}}E_O=\hat{E}_{\mathrm{SB}}$, $m_O=\hat{p}$, $n_O=\hat{q}$,$r_O=1$.

Once the vector $\underline{\hat{\vartheta}}''=[\hat{r}\hat{c}\hat{d}\hat{m}\hat{n}]$ has been determined, the final values of $\hat{z}$, $\hat{A}_{\mathrm{GSB}}$, and $\hat{E}_{\mathrm{GSB}}$ are calculated by means of the inverse formulas which is possible to derive from Eqs. 12, 17, and 18.

It is worth to stress that the initial condition $\alpha(0)=\alpha_0\neq 0$ is required only during the identification phase where it is used for the prior identification of the SB(p,q) model and for the scaling of z (Eq. 11).

The method of identification of the GSB model discussed above will be illustrated in the successive sections considering both numerical simulations and real experimental data.

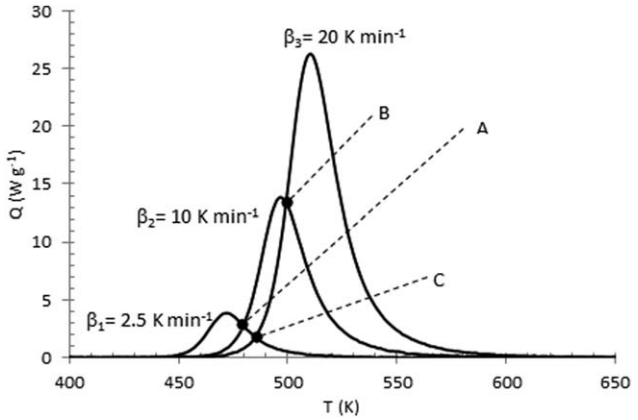

Figure 2. Heat power curves gathered during the numerical experiments carried out under dynamic conditions at $\beta_1=2.5$, $\beta_2=10$, and $\beta_3=20$ K min^{-1} (values reported near the respective curve) considering the GSB(z, m, n) model.

Numerical Experiments

With the aim of illustrating the procedures described above a series of numerical experiments were performed using Matlab software.[20] Differential equations were integrated using Simulink[20] [ode15s (Stiff/NDF) solver] and the minimization procedure implemented by means of specific programs using the commands *lsqnonlin* for the minimization algorithms and *nlparci* for the error bounds evaluations. These software tools were used also for the treatment of the real experimental data. Figure 2 report the results of a set of numerical experiments performed considering Eq. 5 integrated under dynamic conditions ($T=T_O+\beta t$) with $T_{\mathrm{O}}=400$ K, for three different values of the heating rate ($\beta_1=2.5$, $\beta_2=10$ and $\beta_3=20$ K min^{-1}) and considering for the Arrhenius and GSB(z,m,n) model parameters those used to gather the results reported in Figure 1 ($A_{\mathrm{GSB}}=10^{+9}\mathrm{s}^{-1}$, $E_{\mathrm{GSB}}=100,000\,\mathrm{J\,mol}^{-1}$, $m=0.75$, $n=2$, and $-\Delta H_R=2500\,\mathrm{J\,g}^{-1}$) and assuming $z=10^{-3}$. For $t_{\mathrm{O}}=0$, the initial condition $\gamma(0)=0$ has been assumed in all the cases. The effect of the experimental error has been taken into account adding to the calculated heat power curves a random Gaussian error with mean 0 and variance $\sigma^2=6.2510^{-4}$.

The first step is the assessment of the parameter of the classic SB(p,q) model that best describe the experimental data. To this end the method proposed by the authors in a previous work has been used.[6] As the heat power curves carried out considering two different heating rates intercept in a point different than the origin (A, B, C in Figure 2) it can be concluded that SB(p,q) model can describe the system under study and the identification procedure should provide: $0<p<1$ and $q>0$. The linear interpolation (Eq. 13c) of the variable $y_{i,j}$ vs. $x_{i,j}$ (Eq. 13a and 13b) carried out for all the possible combination of indexes (i, j) evaluated over suitable evaluation temperature intervals provide a first estimate of the kinetic exponents p and q ($p_{\mathrm{O}}=0.7465$ and $q_{\mathrm{O}}=2.0107$). With these values of the kinetic exponents, a first estimate of the Arrhenius parameter $A_{\mathrm{SB,O}}=2.33\ 10^{+9}$ s^{-1} and $E_{\mathrm{SB,O}}=103{,}403$ J mol^{-1} were determined by means of the application of the extended Kissenger's method (Eq. 14). A successive multivariate OLS procedure then is carried out using the results coming from the identification of the SB(p,q) model. During the identification of the SB(p,q) model, the experimental data considered for the evaluation of the objective function (sum of the squared errors) [$(T,Q_i(T))$and the corresponding $(T,\alpha_i(T))$ curves] were such that $\alpha_i(T)>\alpha_{\mathrm{O}}$ being $\alpha_{\mathrm{O}}=10^{-3}$ the initial condition used for the integration of the heat balance equation 5 evaluated using the SB(p,q) model (Eq. 1).

The final estimate obtained for the SB(p,q) model gave: $\hat{A}_{\mathrm{SB}}=9.7310^{+8}$ s^{-1}, $\hat{E}_{\mathrm{SB}}=99,960\mathrm{Jmol}^{-1}$, $\hat{p}=0.7361$, and $\hat{q}=1.9907$. The initial guess for the identification of the GSB (z,m,n) model were determined using the final estimates of the SB(p,q) model identified. These values were: $c_O=\hat{c}_{\mathrm{SB}}=-3.6902$, $d_O=\hat{d}_{\mathrm{SB}}=0.9667$, $m_O=\hat{p}=0.7361$, $n_O=\hat{q}=1.9907$, and setting $r_O=1$.

The optimization procedure performed considering the reparametrized form of the mass balance equation (Eq. 19) starting from the initial guess of the parameters

$$\underline{\vartheta_0'''}=[r_O,c_0,d_0,m_0,n_0]=[1.000,-3.6902,0.9667,0.7361,1.9907],$$

led to the following final estimate of the model parameter

$$\underline{\hat{\vartheta}}''=[\hat{r},\hat{c},\hat{d},\hat{m},\hat{n}]=[1.0731,-3.6729,1.0013,0.7502,2.0013].$$

Applying the inverse transformations reported in Eq. 11, 12, and 17 the following final estimates were calculated: $\hat{z}=1.0310^{-3}$, $\hat{A}_{\mathrm{GSB}}=1.02\cdot 10^{+9}$ s^{-1}, $\hat{E}_{\mathrm{GSB}}=100,088\,\mathrm{J\,mol}^{-1}$; considering that the final estimates of the kinetic exponents of the GSB model are: $\hat{m}=0.7502$, $\hat{n}=2.0013$, it can be concluded that the identification procedure provides model parameters estimates which are comparable to the theoretical values used to perform the simulations.

The procedures reported above have been applied considering different values of the GSB(z,m,n) model parameter (Table 1) using the same temperature ramps, the same values for the Arrhenius parameters and the reaction's heat as those used to obtain the results of Figure 2.

Table 2 reports the first estimates of the kinetic exponents of the SB(p,q) model that can be derived with the simulated data obtained with the values of the GSB(z,m,n)reported in Table 1, by interpolation (Eq. 13c) of the variables calculated considering the Eq. 13a and 13b. Figure 3 shows an

Table 1. Parameter Used for the Simulation of the GSB(z, m, n) Model

Model	z	m	n
1	10^{-5}		
2	10^{-3}	0.75	1.00
3	10^{-1}		
4	10^{-5}		
5	10^{-3}	0.75	2.00
6	10^{-1}		
7	10^{-5}		
8	10^{-3}	0.50	2.00
9	10^{-1}		
10	10^{-5}		
11	10^{-3}	0.50	1.00
12	10^{-1}		

example of these calculations carried out for the models 2, 8, and 11 of Table 1.

Table 3 reports both the first estimates and the final values of the parameters collected during the SB(p,q) model identification procedure. In all the cases, an initial conversion $\alpha_O = 10^{-3}$ was considered for the integration of the Eq. 6.

From the final estimates reported in Table 3 assumed as initial guess for the parameters of the GSB(z, m, n) model, the final estimations of the kinetic triplet have been determined (Table 4).

Table 2. Initial Estimates of the Kinetic Exponents Obtained During the Identification of the SB(p,q) Model Considering the True Parameters Reported in Table 1 for the GSB(z, m, n) Simulations

Model	Index combinations	Evaluation Temperature Intervals (K)	p	q
	(1, 2)	472–488	0.7509	1.0023
1	(2, 3)	482–518	0.7622	1.0145
	(1, 3)	483–488	0.7511	1.0028
	(1, 2)	467–486	0.7444	0.9991
2	(2, 3)	474–516	0.7521	1.0125
	(1, 3)	473–486	0.7328	0.9875
	(1, 2)	452–476	0.5152	0.9250
3	(2, 3)	456–507	0.5187	0.9848
	(1, 3)	453–476	0.4576	0.8714
	(1, 2)	478–492	0.7457	1.9928
4	(2, 3)	487–538	0.7564	2.0050
	(1, 3)	489–492	0.7583	2.0129
	(1, 2)	474–491	0.7498	2.0119
5	(2, 3)	483–537	0.7353	1.9922
	(1, 3)	483–491	0.7545	2.0279
	(1, 2)	452–484	0.5110	1.9010
6	(2, 3)	456–532	0.5376	1.9859
	(1, 3)	456–484	0.4579	1.8199
	(1, 2)	454–483	0.4925	1.9864
7	(2, 3)	460–534	0.5128	2.0126
	(1, 3)	460–483	0.4964	1.9890
	(1, 2)	454–483	0.4909	1.9857
8	(2, 3)	460–534	0.5116	2.0125
	(1, 3)	459–483	0.4954	1.9892
	(1, 2)	446–481	0.3906	1.9649
9	(2, 3)	448–530	0.4199	2.0082
	(1, 3)	448–481	0.3714	1.9340
	(1, 2)	454–476	0.4978	1.0002
10	(2, 3)	460–508	0.5025	1.0040
	(1, 3)	459–476	0.4992	1.0006
	(1, 2)	453–477	0.4984	1.0003
11	(2, 3)	460–508	0.5026	1.0049
	(1, 3)	459–476	0.4982	0.9994
	(1, 2)	444–473	0.3932	0.9746
12	(2, 3)	445–504	0.3986	0.9977
	(1, 3)	445–473	0.3740	0.9549

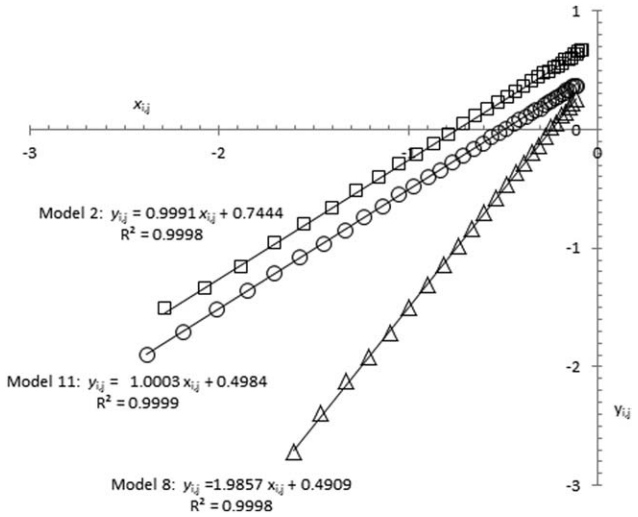

Figure 3. Regression lines (Eq. 13c) obtained plotting $y_{i,j}$ (Eq. 13b) vs. $x_{i,j}$ (Eq. 13a) considering the case 2, 8 and 11 of Table 1 for $(i, j) = (1, 2)$ (See Table 2) (Equations and correlation coefficients are reported near the respective curves).

In each case, the analysis of the final estimates $\underline{\hat{\vartheta}}_{\mathrm{GSB}} = [\hat{z}, \hat{A}_{\mathrm{GSB}}, \hat{E}_{\mathrm{GSB}}, \hat{m}, \hat{n}]$ reported in Table 4 clearly shows a good agreement with the true model parameters reported in Table 1. It is worth noting that similar results (not reported) have been gathered using different values both of the Arrhenius, (z, m, n) parameters and initial conversion α_O confirming the generality of the approach.

Experimental

Nitroaromatic compounds are widely used in the chemical industry for the production, just citing a few, of explosives, dyes, pharmaceutical and pesticides.[21] Despite their common use, incidents continue to be recorded especially for their tendency to trigger dangerous thermal decomposition processes with a huge heat and gas evolution. The thermal decomposition of nitro compounds is generally triggered by the omolytic scission of the C—NO_2 bond or more complex processes involving the interaction of vicinal groups in the case of aromatic molecules, followed by a complex chain propagation process.[22,23] 3,5-dinitro-4-methylbenzoic acid (CAS: 16533-71-4) is a yellow crystalline powder, stable at ambient temperature melting at about 428–431 K which is also used for analytical purposes.[24,25]

Samples were purchased from Sigma Aldrich (purity 98 w/w-%) and DSC experiments were performed both under dynamic and isothermal conditions using a PerkinElmer DSC 8000 calorimeter equipped with an Intracooler II cooling system. The system was calibrated using as calibration standard indium. DSC runs were carried out on samples of 0.5–0.8 mg using Stainless Steel High Pressure capsules (PerkinElmer part n. B018 2901) and adopting, for the dynamic experiments temperature ramps started at 413 K with heating rates of 2.5, 10, and 20 K min^{-1}. Isothermal experiments were performed at 518, 533, and 553 K using the same high capsules used for the dynamic experiments. Each run was repeated three times both under dynamic and isothermal conditions and the mean curves were used in all the successive calculations.

Table 3. Initial Estimates ($d_{SB,O}=1$ in each Case) and Final Values Concerned with the Identification of the SB(p,q) Model Using the Simulated Data of the GSB(z,m,n) Models of Table 1

Model	$c_{SB,O}$	p_O	q_O	$\hat{c}_{SB}$	$\hat{d}_{SB}$	$\hat{p}$	$\hat{q}$
1	−3.7163	0.7547	1.0066	−3.5765	1.0000	0.7470	0.9998
2	−3.4717	0.7431	0.9997	−3.6562	1.0000	0.7383	0.9957
3	−4.2523	0.4972	0.9271	−4.2569	0.9877	0.4797	0.9084
4	−3.5096	0.7535	2.0036	−3.6188	1.0189	0.7467	1.9973
5	−3.6594	0.7465	2.0107	−3.6903	0.9669	0.7361	1.9908
6	−4.3050	0.5022	1.9023	−4.3338	1.0200	0.4587	1.8466
7	−4.2358	0.5006	1.9960	−4.2462	0.9885	0.4993	1.9964
8	−4.2270	0.4993	1.9958	−4.2628	0.9835	0.4962	1.9948
9	−4.4469	0.3940	1.9690	−4.4535	0.9980	0.3710	1.9380
10	−4.2309	0.4988	0.9984	−4.1881	0.9869	0.4988	0.9984
11	−4.2107	0.4997	1.0015	−4.1976	0.9745	0.4972	0.9983
12	−4.3904	0.3886	0.9757	−4.4421	1.0215	0.3778	0.9646

Table 4. Final Estimate of the Arrhenius and GSB(z,m,n) Model Parameter Gathered Considering the Estimated SB(p,q) Model

Model	$\hat{z}$	$\hat{A}_{GSB}(s^{-1})$	$\hat{E}_{GSB}(Jmol^{-1})$	$\hat{m}$	$\hat{n}$
1	$7.63\ 10^{-6}$	$1.02\ 10^{+9}$	100,072	0.7491	1.0010
2	$9.76\ 10^{-4}$	$1.02\ 10^{+9}$	100,071	0.7490	1.0008
3	$1.00\ 10^{-1}$	$9.99\ 10^{+8}$	100,001	0.7498	0.9991
4	$7.03\ 10^{-6}$	$1.02\ 10^{+9}$	100,085	0.7484	1.9986
5	$1.03\ 10^{-3}$	$1.02\ 10^{+9}$	100,088	0.7502	2.0013
6	$9.98\ 10^{-2}$	$1.00\ 10^{+9}$	100,022	0.7485	1.9996
7	$4.80\ 10^{-5}$	$9.87\ 10^{+8}$	99,945	0.5008	1.9984
8	$1.11\ 10^{-3}$	$9.87\ 10^{+8}$	99,944	0.5009	1.9984
9	$9.72\ 10^{-2}$	$9.53\ 10^{+8}$	99,799	0.4984	1.9972
10	$3.55\ 10^{-5}$	$9.98\ 10^{+8}$	99,993	0.5002	1.0001
11	$9.42\ 10^{-4}$	$9.97\ 10^{+8}$	99,988	0.4998	1.0001
12	$9.77\ 10^{-2}$	$1.00\ 10^{+9}$	100,007	0.4962	0.9996

Dynamic DSC experiments

Figure 4 shows an example of dynamic DSC heat power signal collected during a dynamic DSC run carried out on a sample of 3,5-dinitro-4-methylbenzoic acid using a heating rate of $\beta = 2.5$ K min^{-1}. Baseline was evaluated using the tangential area-proportional method and has allowed the assessment of the subtracted peak (left scale) and of the corresponding conversion (right scale): $\alpha = \frac{\int_0^t Q(t)dt}{-\Delta H_R}$ with: $-\Delta H_R = \int_0^{\infty} Q(t)dt = \frac{1}{\beta}\int_{T_O}^{T_{end}} Q(T)dT$

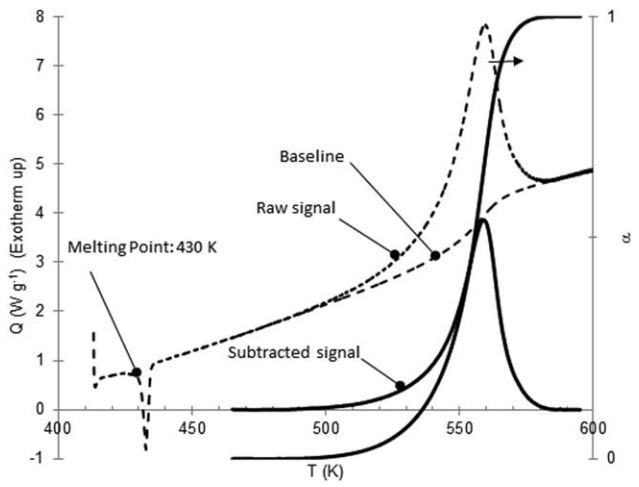

Figure 4. Experimental, tangential area-proportional baseline and subtracted peak (left scale) along with its corresponding conversion curve (Right scale) in a dynamic DSC run carried out on a sample of 3,5-dinitro-4-methylbenzoic acid at $\beta = 2.5$ K min^{-1}.

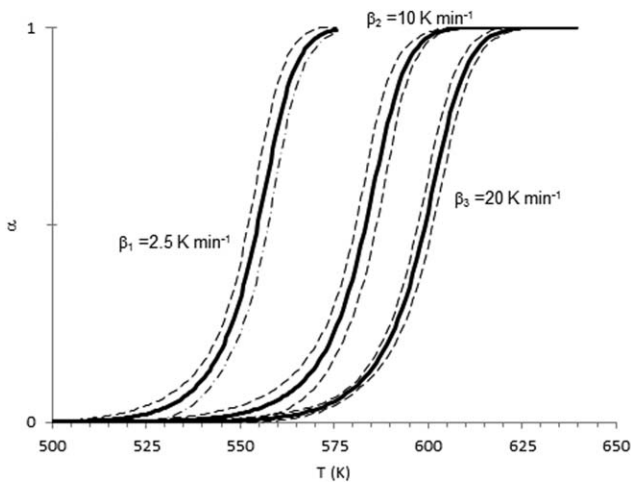

Figure 5. Mean experimental conversions (solid lines) along with their 95 % confidence bands (dashed lines) gathered during the DSC dynamic experiments (Heat rates reported near the respective curves) carried out on 3,5-dinitro - 4-methylbenzoic acid.

Table 5. Initial Estimates of the Kinetic Exponents Obtained During the Thermal Decomposition of 3,5-dinitro-4-methylbenzoic Acid Using the SB(p,q) Model

Index Combinations	Evaluation Temperature Intervals (K)	p	q
(1, 2)	554–567	0.74	0.95
(2, 3)	563–603	0.75	1.04
(1, 3)	563–566	0.73	1.07

Figure 5 reports the mean conversion curves along with the corresponding 95% confidence bands collected during the dynamic DSC runs carried out on the system under study.

From the integration of the DSC peaks a reaction heat of $-\Delta H_{R,dyn} = 2{,}038 \pm 192$ J g^{-1} was calculated. The linear interpolation (Eq. 13c) carried out on the variables calculated considering Eq. 13a and 13b was applied to all the possible couples of curves allowing the determination of an estimate of the kinetic exponent p and q reported in Table 5. Considering the mean of the values reported in Table 5, it is possible to calculate the following first estimate of the kinetic exponents of the SB(p,q) model: $p_O = 0.74$ and $q_O = 1.02$. With these values and applying the extended Kissinger's method (Eq. 14) a first estimate of the activation energy $E_{SB,O} = 119{,}025$ J mol^{-1} and a pre-exponential factor $A_{SB,O} = 1.53 \cdot 10^{+9}$ s^{-1} were estimated. The first estimate of the parameter $c_{SB,O}$ calculated using Eq. 16 ($T_{ref} = 581$ K) yielded: $c_{SB,O} = -4.07$. The final values of the parameters collected after the SB(p,q) model identification procedure (also in this case an initial conversion $\alpha_O = 10^{-3}$ for the integration of the Eq. 6 was considered) were: $\hat{c}_{SB} = -3.88$, $\hat{d}_{SB} = 0.98$ $\hat{p} = 0.73$, and $\hat{q} = 0.92$. Considering these values as the first estimate for the GSB(z,m,n) identification: $c_{GSB,O} = \hat{c}_{SB}$, $d_{GSB,O} = \hat{d}_{SB}$, $m_O = \hat{p}$, $n_O = \hat{p}$ and assuming $r_O = 1$, at the end of the multivariate OLS identification procedure, the final estimates reported in Table 6 along with the respective 95% error bounds were determined. The error bounds for the parameters were calculated reoptimizing the identified parameters by removing their centering and scaling (*Matlab* command: *lsqnonlin*[20]). This procedure provides the parameter values, the vector of residuals and the Jacobian matrix at the minimum. The use of *Matlab* command *nlparci*[20] which require the knowledge of the parameter estimates and of the Jacobian and the residuals at the minimum of the objective function, allowed the estimation of the 95% confidence intervals for the parameters.

Table 6. Final Estimate of the Arrhenius and GSB(z,m,n) Model Parameters Along with Their 95% Confidence Intervals in the Case of the Thermal Decomposition of 3,5-dinitro-4-methylbenzoic Acid

Parameter	Mean Value	95% Confidence Interval
$\hat{z}$	0.029	0.002
$\hat{A}_{GSB}$	1.31 10^{+9}	3.15 10^{+7}
$\hat{E}_{GSB}$	118525	196
$\hat{m}$	1.133	0.035
$\hat{n}$	1.091	0.022

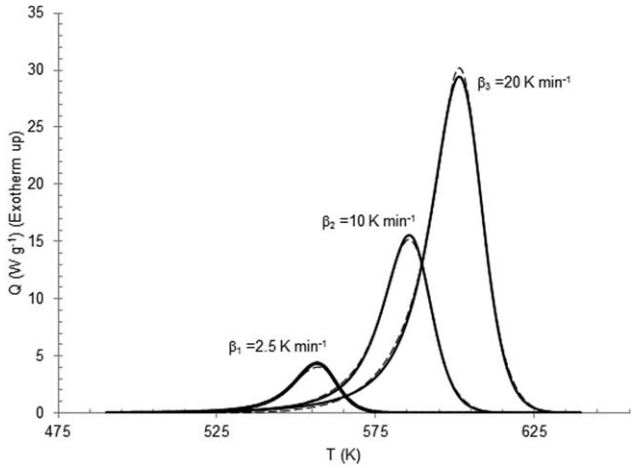

Figure 6. Experimental (dashed) and calculated (solid) results collected during the dynamic DSC experiment carried out on 3,5-dinitro-4-methylbenzoic acid at 2.5, 10, and 20 K min^{-1} (values reported near the respective curves).

It is worth observing that the restriction valid for the first exponent of the SB(p,q) model: $0 < p < 1$, does not hold in the case of the GSB(z,m,n)model.

Figure 6 reports the experimental DSC data and the calculated curves evaluated using the parameters reported in Table 6.

It is worth to observe that the *multicollinearity* of the parameters is greatly reduced by means of the centering and scaling performed by means of the Eqs. 11 and 15. In fact, these transformations lead to the determination of a Hessian matrix $H\left(H=(h_{i,j}) : h_{i,j}=\frac{\partial^2 \Psi}{\partial \vartheta_i \partial \vartheta_j}\right)$ that shows at the minimum $\vartheta = \underline{\hat{\vartheta}}$ the minimum value of the so called spread number[19] defined as $N(H) = \ln(\lambda_{max}) - \ln(\lambda_{min})$ (λ_{min} and λ_{max} are, respectively, the maximum and minimum eigenvalue of H). In our case, N resulted equal to 9.5 for the scaled and centered parameters and 47.4 for the original ones.

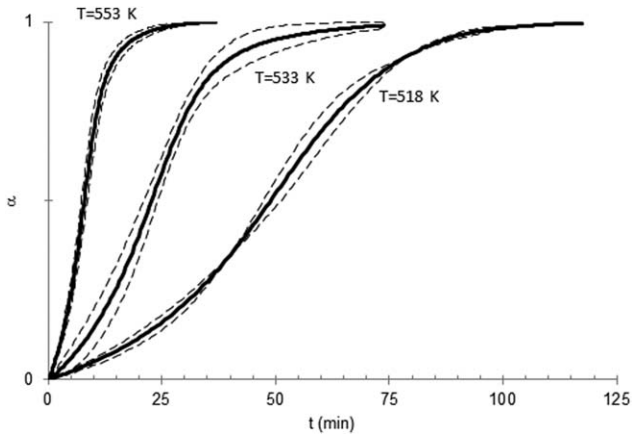

Figure 7. Mean Conversion curves (Continuous lines) along with their respective 95% confidence bands (dashed lines), collected during the isothermal decomposition of 3,5-dinitro-4-methylbenzoic acid (temperatures are reported near the respective curves).

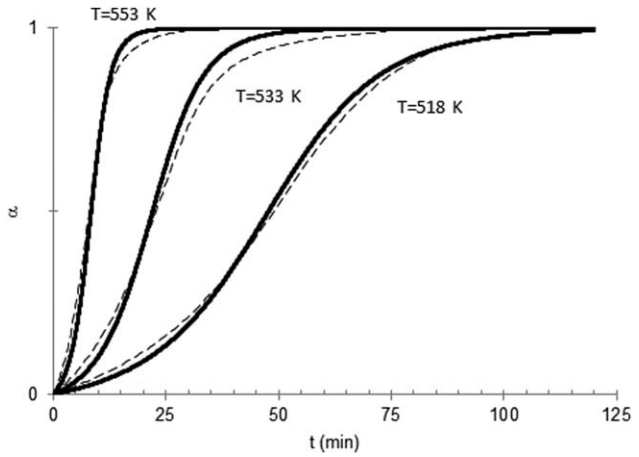

Figure 8. Calculated curves generated using the identified GSB(z,m,n)model (continuous line) and the corresponding mean experimental curves (dashed lines) gathered during the thermal decomposition 3,5-dinitro-4-methylbenzoic acid under isothermal conditions.

Isothermal DSC experiments

Figure 7 reports the mean conversion curves along with the corresponding 95% confidence bounds collected during the isothermal DSC experiments concerned with the thermal decomposition of 3,5-dinitro-4-methylbenzoic acid.

The heat of decomposition evaluated under isothermal conditions resulted: $-\Delta H_{R,Iso} = 2.155 \pm 405$ J g which is comparable to that evaluated under dynamic conditions.

Figure 8 shows the isothermal curves obtained using the GSB(z,m,n) obtained from the dynamic DSC experiments (Table 6) along with the corresponding experimental results.

The analysis of Figure 8 demonstrates a satisfactory agreement among experimental data and theoretical predictions. It is worth stressing that the identifications performed considering different values of the initial conversion $\hat{n}$ ($0.5\ 10^{-5}$, 10^{-4}, and 10^{-2}) allowed to determine in each case the same mean values as those reported in Table 6.

Conclusions

The thermal decomposition of 3,5-dinitro-4-methylbenzoic acid has been studied by means of DSC techniques and its behavior has been satisfactorily described using the generalized form of the Šesták–Berggren model. It has been shown that the use of the generalized autocatalysis model (Eq. 4) can lead to inaccurate conclusions if the role of the initiation parameter z is not properly taken into account. It has been shown that, due to the extreme sensitivity of the model response with respect to this parameter, the parameter z should be carefully estimated along with the other kinetic and Arrhenius parameters. A procedure devoted to the identification of the complete kinetic triplet has been developed starting from the knowledge of the Arrhenius parameters and kinetic exponents that can be derived using the classic two parameters Šesták–Berggren's model. An expression linking the initialization parameter z with the SB(p,q) model previously identified has been derived and successfully used during the identification procedure of the GSB(z,m,n)model. The identified parameters have been used to simulate the system behavior under isothermal conditions and the results compared with real DSC experiments. A good agreement among simulated and real data has been observed demonstrating the validity of the approach.

Acknowledgment

The author would like to thank Mr Andrea Bizzarro for his Technical support.

Notation

Roman symbols

A = apparent pre-exponential factor, s^{-1}
c = parameter in Eq. 16
d = parameter in Eq. 16
E = apparent activation energy, J mol^{-1}
f(α) = kinetic model, dimensionless
GSB(z,m,n) = Generalized Šesták–Berggren model with parameters z, m and n
H = Hessian matrix
K(T) = apparent kinetic constant, s^{-1}
m = first exponent in the generalized GSB model, dimensionless
n = second exponent in the generalized GSB model, dimensionless
N = Spread number
p = first exponent in the SB model, dimensionless
q = second exponent in the SB model, dimensionless
Q = specific heat power, W g^{-1}
r = parameter in Eq. 12
R = 8.314 = gas constant, J mol^{-1} K^{-1}
RO(v) = reaction order model
SB(p, q) = Šesták–Berggren model with exponents p and q
t = time,seconds (s) or minutes (min)
T = temperature, K
T_{Ref} = reference temperature, K
x = variable in Eq. 12a, dimensionless
y = variable in Eq. 12b, dimensionless
z = initialization parameter in Eq. 4, dimensionless

Greek letters

α, γ = conversion degree, dimensionless
β = heat rate, K min^{-1}
ΔH_R = heat of reaction, J g^{-1}
Γ = curve on the plane (T, q)
λ = eigenvalue
v = exponent in the reaction order model, dimensionless
σ^2 = variance
$\underline{\hat{\vartheta}}$ = Vector of parameters
Ψ = Objective function (Sum of Squared Errors)

Other symbols

$\wedge$ = on a symbol means: estimated parameter
o = as subscript means: Initial value or estimation
$\forall$ = means: for each universal quantifier
SB = as subscript means: parameter referred to the SB(p, q) model
GSB = as subscript means: parameter referred to the GSB(z,m,n)model

Literature Cited

1. Bou-Diab L, Fierz H. Autocatalytic decomposition reactions, hazards and detection. *J Hazard Mater*. 2002;93:137–146.
2. Chervin S, Bodman GT. Phenomenon of autocatalysis in decomposition of energetic chemicals. *Thermochim Acta*. 2002;392–393:371–383.
3. Kidam K, Hurme M. Statistical analysis of contributors to chemical process accidents. *Chem Eng Technol*. 2013;36(1):167–176.
4. Wang Q, Rogers WJ, Mannan MS. Thermal risk assessment and rankings for reaction hazards in process safety. *J Therm Anal. Calorim*. 2009;98:225–233.
5. Sales J, Mushtaq F, Christou MD, Nomen R. Study of major accidents involving chemical reactive substances: analysis and lessons learned, *Process Saf Environ Protec*. 2007;85(2):117–124.

6. Sanchirico R. Model selection and parameters estimation in kinetic thermal evaluations using semiempirical models. *AIChE J*. 2012; 58(6):1869–1879.
7. Šesták J, Berggren G. Study of the kinetics of the mechanism of solid-state reactions at increasing temperatures. *Thermochim Acta*. 1971;3:l–12.
8. Šimon P. Fourty years of the Šesták–Berggren equation. *Thermochim Acta*. 2011;520:156–157.
9. Sanchirico R. Adiabatic behavior of thermal unstable compounds evaluated by means of dynamic scanning calorimetric (DSC) techniques. *AIChE J*. 2013;59(10):3806–3815.
10. ASTM E2070; Standard Test Method for Kinetic Parameters by Differential Scanning Calorimetry Using Isothermal Methods. *Annual Book of ASTM Standards*, American Society for Testing and Materials, West Conshohocken, PA, 2001.
11. Brown ME, Maciejewski M, Vyazovkin S, Nomen R, Sempere J, Burnham A, Opfermann J, Strey R, Anderson HL, Kemmler A, Keuleers R, Janssens J, Desseyn HO, Li CR, Tang TB, Roduit B, Malek J, Mitsuhashi T. Computational aspects of kinetic analysis Part A: The ICTAC kinetics project-data, methods and results. *Thermochim Acta*. 2000;355:125–143.
12. Wilcock E, Rogers RL. A review of the phi factor during runaway conditions. *J Loss Prev Process Ind*. 1997;10(5–6):289–302.
13. Burnham AK. Application of the Šesták–Berggren Equation to Organic and Inorganic Materials of Practical Interest. *J Therm Anal Calorim*. 2000;60:895–908.
14. Šimon P. Considerations on the single-step kinetics approximation. *J Therm Anal Calorim*. 2005;82:651–657.
15. Kossoy AA, Hofelich T. Methodology and software for reactivity rating. *Process Saf Prog*. 2003;22(4):235–240.
16. Pratap A, Shanker Rao TL, Lad KN, Dhurandhar HD. Isoconversional vs. model fitting methods, a case study of crystallization kinetics of a Fe-based metallic glass. *J Therm Anal Calorim*. 2007; 89(2):399–405.
17. Llòpiz J, Romero MM, Jerez A, Laureiro Y. Generalization of the kissinger equation for several kinetic models. *Thermochim Acta*. 1995;256:205–211.
18. Chen D, Gao X, Dollimore D. A generalized form of the Kissinger equation. *Thermochim Acta*. 1993;215:109–117.
19. Rodionova OE, Pomerantsev AL. Estimating the Parameters of the Arrhenius Equation. *Kinet Catal*. 2005;46(3):305–308.
20. Mathworks, Matlab, Software for Scientific Computing, online Manuals and Additional Material. Available at: http://www.mathworks.-com/. Accessed on: September 2014.
21. Ju KS, Parales RE. Nitroaromatic Compounds, from Synthesis to Biodegradation. *Microbiol Mol Biol Rev*. 2010;74(2):250–272.
22. Furman D, Kosloff R, Dubnikova F, Zybin SV, Goddard WA, Rom N, Hirshberg B, Zeiri Y. Decomposition of condensed phase energetic materials: interplay between uni-and bimolecular mechanisms. *J Am Chem Soc*. 2014;136:4192−4200.
23. Brill TB, James KJ. Kinetics and mechanisms of thermal decomposition of nitroaromatic explosives. *Chem Rev*. 1999;03:2667–2692.
24. Preiss A, Elend M, Gerling S. Identification of highly polar nitroaromatic compounds in leachate and ground water samples from a TNT-contaminated waste site by LC-MS, LC-NMR, and off-line NMR and MS investigations. *Anal Bioanal Chem*. 2007;389(6): 1979–1988.
25. Trost BM, Ameriks MK. Pd-catalyzed carbonylative lactamization: a novel synthetic approach to FR900482. *Org Lett*. 2004;6(11):1745–1748.

Manuscript received Sept. 12, 2014, and revision received Nov. 13, 2014.